

Review

Timea Frosch, Andreas Knebl and Torsten Frosch*

Recent advances in nano-photonic techniques for pharmaceutical drug monitoring with emphasis on Raman spectroscopy

<https://doi.org/10.1515/nanoph-2019-0401>

Received October 4, 2019; revised November 9, 2019; accepted November 18, 2019

Abstract: Innovations in Raman spectroscopic techniques provide a potential solution to current problems in pharmaceutical drug monitoring. This review aims to summarize the recent advances in the field. The developments of novel plasmonic nanoparticles continuously push the limits of Raman spectroscopic detection. In surface-enhanced Raman spectroscopy (SERS), these particles are used for the strong local enhancement of Raman signals from pharmaceutical drugs. SERS is increasingly applied for forensic trace detection and for therapeutic drug monitoring. In combination with spatially offset Raman spectroscopy, further application fields could be addressed, e.g. *in situ* pharmaceutical quality testing through the packaging. Raman optical activity, which enables the thorough analysis of specific chiral properties of drugs, can also be combined with SERS for signal enhancement. Besides SERS, micro- and nano-structured optical hollow fibers enable a versatile approach for Raman signal enhancement of pharmaceuticals. Within the fiber, the volume of interaction between drug molecules and laser light is increased compared with conventional methods. Advances in fiber-enhanced Raman spectroscopy point at the high potential for continuous online drug monitoring in clinical therapeutic diagnosis. Furthermore, fiber-array based non-invasive Raman spectroscopic chemical imaging of tablets might find application in the detection

of substandard and counterfeit drugs. The discussed techniques are promising and might soon find widespread application for the detection and monitoring of drugs in various fields.

Keywords: nano-photonic technologies; Raman spectroscopy; pharmaceuticals; drugs; fiber-enhanced Raman spectroscopy (FERS); hollow-core photonic crystal fiber; nano-structured fiber sensors; surface-enhanced Raman spectroscopy (SERS); spatially offset Raman spectroscopy (SORS); Raman optical activity (ROA); Raman chemical imaging; drug sensing; therapeutic drug monitoring (TDM); body fluid; urine; plasma; serum; saliva; anti-infectives; antibiotics; anti-cancer drugs; process monitoring; enantioselective Raman spectroscopy (EsR).

1 Introduction

Drug monitoring is highly important for different fields: medical diagnostics, forensics, and process analytics. Currently established techniques fail to meet the demands in terms of either speed, sensitivity, or out-of-the-lab applicability. Novel chemically selective nano-photonic techniques could offer a solution to present problems.

Globally, severe diseases are among the main causes of death [1]. Accessible and simple analytical tools for the early diagnosis and accurate therapy of diseases are thus crucial. Appropriate treatment of life-threatening diseases like cancer and sepsis depends on precise and early diagnosis and therapy follow-ups to determine the success of the medication. For cancer, chemotherapy is widely applied for various malignancies, using diverse anti-cancer drugs with different pharmacologic profiles. One characteristic is common: it is very difficult to find the right dose regimen for an individual patient. High doses can induce severe side effects, which reduces the patient's quality of life, but often improve the prognosis and the outcome [2]. Every case is unique, as each patient has her or his personal pharmacokinetic profile, which defines

*Corresponding author: **Torsten Frosch**, Leibniz Institute of Photonic Technology, 07745 Jena, Germany; Friedrich Schiller University, Institute of Physical Chemistry, 07743 Jena, Germany; and Friedrich Schiller University, Abbe Center of Photonics, 07745 Jena, Germany, e-mail: torsten.frosch@uni-jena.de, torsten.frosch@gmx.de.
<https://orcid.org/0000-0003-3358-8878>

Timea Frosch: Leibniz Institute of Photonic Technology, 07745 Jena, Germany

Andreas Knebl: Leibniz Institute of Photonic Technology, 07745 Jena, Germany; and Max Planck Institute for Biogeochemistry, 07745 Jena, Germany

the treatment efficiency. Recent clinical studies prove the great value of individualized medical treatment [3, 4].

Individualized treatment would also benefit the large number of patients suffering from sepsis. Sepsis is a dys-regulated host response to infection, which can cause life-threatening organ dysfunctions and is associated with high mortality rates [5, 6]. Within the last years, it became clear that standard dose recommendations, which are derived from studies with healthy volunteers or patients with mild or moderate infections, cannot be transferred to critically ill patients with severe infections [7, 8]. For some anti-infectives, dose adjustment based on therapeutic drug monitoring (TDM) has already been shown to improve the clinical outcome [9–12].

Techniques that are currently employed in the clinics to determine the antibiotic or anti-cancer drug levels in body fluids of patients are mainly based on chromatography and electrophoresis, frequently coupled with mass-spectrometric detection. These methods are time consuming and require complex procedures for sample preparation. The time-to-result interval also includes sample transport to central hospital labs and is in the range of several hours. Immediate and continuous dose adjustment is thus impossible, which hinders an optimal outcome for critically ill patients. Quick, highly chemically selective and sensitive innovative photonic technologies could enable the necessary rapid detection of antibiotic or anti-cancer drug levels in patients.

Besides the medical field, forensics would also benefit from the application of photonic approaches for drug monitoring in body fluids that allow rapid analysis and on-site application.

Additionally to these application fields, chemically selective on-site methods are highly desired as process analytical technologies (PAT) in pharmaceuticals [13–15]. Mistakes in the fabrication of pharmaceuticals are currently only detected at the very end of the production process. A chemically selective in-line analysis in early production steps would be of great advantage to control the process and save scrap costs.

Nano-photonic sensors show the potential to meet the above-mentioned requirements. This is particularly true for sensors based on Raman spectroscopy. Recent developments in nano-structured sensor techniques strongly improved the power of Raman sensing and opened up new paths for promising applications in drug monitoring. Thus, nano-photonic sensors are on the road to become an alternative to established costly, bulky, and strictly lab-based techniques. This trend is also reflected in the published scientific literature (Figure 1). According to Web of Science statistics, the number of articles published per

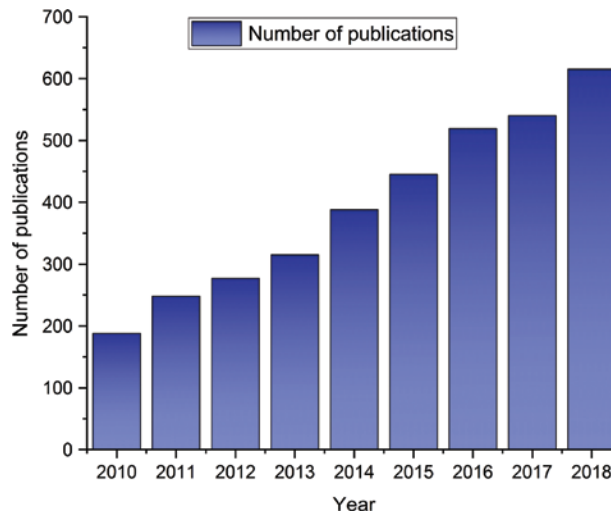


Figure 1: Evolution of the number of publications containing the keywords “Raman” and “drug” in the Web of Science database as of June 21, 2019.

year with topics including “Raman” and “drug” more than doubled between 2010 and 2016 and continues to grow. This article reviews recent developments in the field of (nano-)photonic drug monitoring with a focus on Raman spectroscopy.

Raman spectroscopy is a direct optical method based on inelastic light scattering [16] (Figure 2). When light with frequency ω_0 (e.g. laser light) interacts with sample molecules, most photons will be elastically scattered (Rayleigh scattering) without a change in frequency. A small part of the scattered photons will undergo a change in energy and thus frequency ($\omega_s = \omega_0 - \omega_r$ for Stokes Raman scattering and $\omega_s = \omega_0 + \omega_r$ for anti-Stokes Raman scattering). In this case, the molecule ends up in an altered vibrational-rotational state after the scattering process, and the change in frequency of the photon corresponds to the difference between the initial and the final energy levels of the molecule. Vibrations and energy levels are highly specific. The pattern of the overall frequency shifts, the Raman spectrum, is therefore unique for every molecule. Equation (1) expresses the variables contributing to the Stokes-Raman scattering intensity: the excitation frequency ω_0 , the frequency of the Raman scattered light ω_r , the excitation intensity (laser power) I_0 , the number of molecules N which interact with the laser light, and the polarizability of the molecule α .

$$I_{\text{Stokes}} \propto NI_0 (\omega_0 - \omega_r)^4 |\alpha|^2 \quad (1)$$

As an optical, chemically selective method, Raman spectroscopy allows the identification and quantification of numerous molecules simultaneously in different

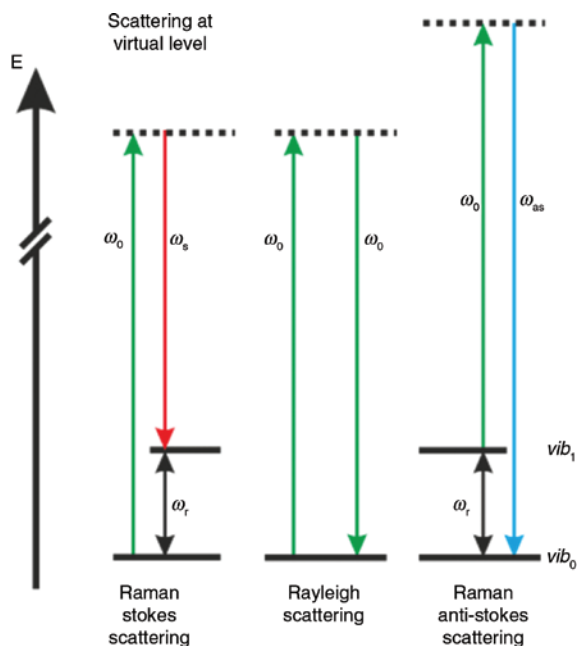


Figure 2: Energy level diagram displaying the principle of the Raman effect: incoming monochromatic light with frequency ω_0 is scattered either elastically (Rayleigh; ω_0) or inelastically with energy transfer to (Raman Stokes scattering; ω_s) or from (Raman anti-Stokes scattering; ω_{as}) the molecule.

The scattered photon consequently has a decreased frequency $\omega_s = \omega_0 - \omega_r$ or increased frequency $\omega_{as} = \omega_0 + \omega_r$. ω_r is the energy difference between the two vibrational levels vib_0 and vib_1 and the respective rotational levels. Adapted from Knebl et al. [17], reproduced with the kind permission of Elsevier, Copyright (2018) Elsevier.

media in a non-destructive way [18–27]. Thanks to recent advances in instrumentation, portable devices [28–32] are available and applied on-site, e.g. for drug sensing [33–39] in forensics [28, 29, 31, 40] and in the pharmaceutical industry [32]. For example, transmission Raman-based methods enable at-line or on-line analysis of bulk content of tablets [41–43] or active pharmaceutical ingredients (APIs) of other solid dosage forms [44]. This technique reached a high level of applicability [44]: cost-savings have been demonstrated in real-world use [45], and considerations for regulatory submission are being discussed [46] for pharmaceutical applications. However, conventional Raman scattering is a very weak process, limiting its use in on-site and point-of-care applications. This is especially true for approaches based on simple portable devices with low sensitivity. To reach the high sensitivities required in applications such as TDM, it is essential to take advantage of enhancement techniques. The Raman signal intensity can be increased by decreasing the excitation wavelength (ω_0) and by increasing the excitation intensity (I_0) or the

number of molecules (N) which interact with the incoming laser light [47].

2 Recent advances in Raman spectroscopic technologies with potential for drug monitoring

2.1 Surface-enhanced Raman spectroscopy for drug monitoring

Simply increasing the laser power to reach high sensitivities is not a valid option as bulky high-power lasers are not practical for on-site or bed-side application. Instead, micro- and nano-structured materials are employed to make the best use of the available laser power. One way is to locally enhance the optical field via the surface plasmon resonance effect. This localized electromagnetic field enhancement is achieved when the wavelength of the illuminating light is resonant with the plasmon frequency of a nano-scaled metal structure [48–50]. The Raman signal of sample molecules in the close vicinity of the metal structure is consequently strongly enhanced. The method based on this local but high Raman signal enhancement is called surface-enhanced Raman spectroscopy (SERS) [51]. An additional enhancement of the Raman signals occurs when molecules are chemisorbed on the SERS-active nano-metals (chemical enhancement), creating new molecular states [52]. Also, colloidal metal solutions can be used as SERS substrates [53].

Nowadays, SERS accounts for approximately 20% of the published articles on Raman drug sensing, according to the Web of Science database (from 298 publications between 2010 and 2018, containing the keywords “Raman” and “drug”, 60 feature “SERS”). Several reviews report on the diverse applications of SERS, e.g. in pharmacy [54–56], for TDM [52, 57], for biological and biomedical applications [58–61], and in forensics [40, 62]. In this review, we focus on advances in SERS with potential towards drug sensing in body fluids which were published after 2017 (see Table 1).

2.1.1 Advances in SERS substrate development for drug sensing applications

For sensing applications, SERS substrates need to provide reproducibly high Raman signal enhancements. Large

Table 1: Recent advances towards SERS-based drug sensing in body fluids.

Reference	Nanoparticle type used as SERS substrate	Drug detected	Lowest detected concentration	Limit of detection (LOD)	Sample medium	Excitation wavelength and laser power	Sample volume
(A) In water or organic solvent							
Yan et al. [63]	Gold (Au) nanoparticles (NP)	3,4-Methylene dioxymethamphetamine	–	10 μM	Water	633 nm, 1 mW	1 μl
Zhao et al. [64]	Silver (Ag) colloid	α -Methyltryptamine Sildenafil	2 mM	1 μM 2 mM	Water Water	785 nm (portable), 90 mW	20 μl
Hong et al. [65]	1D periodic plasmonic Ag structures (nanogratings)	Enrofloxacin	0.17 μM	0.003 μM	Water	785 nm (portable), 250 mW	20 μl
Ding et al. [66]	Colloidal Au NPs	Ciprofloxacin Chloramphenicol	0.037 μM 0.01 μM	0.003 μM 0.01 μM	Aqueous eye-drop solution	785 nm, 0.325 mW	
Saleh et al. [67]	Ag NPs seeded on graphene nanosheets (Ag/G)	2-Thiouracil	10 μM	0.01 μM	Water	633 nm, 1.7 mW	0.75 ml
Tackman et al. [68]	Ag NP (Lee-Meisel)	Chloroquine Doxycycline Primaquine	1 μM 10 μM 0.5 μM	– – –	Aqueous solutions from dissolved dosage forms	633 nm, 50 μW , 785 nm (portable), 50 mW	50 μl
Gao et al. [69]	Ag-Au NP hybrid	1,2-Bis(4-pyridyl)-ethylene	0.1 μM	–	Ethanol	785 nm, 25 mW	10 μl
Haddad et al. [70]	Paper-based substrate impregnated with Ag NP	Cocaine Fentanyl, also in mix heroin	33 μM 0.3 μM	– –	Acetonitrile Methanol	532 nm, 2.5 mW	10 μl
Deng et al. [71]	Au, Ag NP	Aciclovir	50 μM	0.15 μM	Water	785 nm (portable), 500 mW	100 μl
Markina et al. [72]	Calcium carbonate-copper NP	Ceftriaxon Sulfadimethoxine	30 μM 50 μM	<5 μM <5 μM	Water	633 nm, 5 mW	90 μl
(B) In urine							
Meng et al. [73]	2D Au NP-film	Cocaine	– –	1.65 μM 3.3 μM	Urine	633 nm, 1 mW 785 nm (portable), 270 mW	1 ml
Mostowtt and McCord [74]	Au NP	JWH-073 JWH-081 JWH-081 JWH-122	0.76 μM 0.27 μM 0.27 μM 0.28 μM	0.15 μM 0.09 μM 0.09 μM 0.12 μM	Urine	785 nm, 100 mW; (portable: 250 mW)	10 μl
Bindesri et al. [75]	Cotton blend fabric modified with Ag NPs and conductive inks	Levofloxacin	1 mM	–	Urine, synthetic urine	785 nm, 22.3–55.9 mW	10 μl
Markina et al. [76]	Hydroxylamine stabilized Ag NPs (Leopold and Lendl)	Ceftriaxon	9 μM	0.7 μM	Urine	473 nm, 0.5 mW	1 ml

Table 1 (continued)

Reference	Nanoparticle type used as SERS substrate	Drug detected	Lowest detected concentration	Limit of detection (LOD)	Sample medium	Excitation wavelength and laser power	Sample volume
Yu et al. [77]	Au Nanorods (Au NR)	Morphine	0.003 μM	0.003 μM	Urine	785 nm (portable), ca. 250 mW	0.8 ml
Zhu et al. [78]	Ag NP (Lee-Meisel)	Clozapine	1.5 μM	0.3 μM	Urine	785 nm (portable), 200 mW	1 μl
(C) In serum or plasma Berger et al. [79]	Ag NP	Flucytosine	77 μM	93 μM	Undiluted human serum	785 nm (portable), 15 mW	10 μl
Subaihi et al. [80]	Ag NP (Lee-Meisel)	Codein	10 μM	1.39 μM	Human plasma	633 nm, 3 mW	200 μl
Fomasaro et al. [81]	Commercial silicon nanopillars coated with Ag	Imatinib	0.43 μM	0.43 μM	Diluted human plasma	785 nm (portable), 15 mW	60 μl
Yue et al. [82]	Au NPs embedded in composite microparticles	6-Thioguanine	0.2 μM	–	Serum	638 nm (no power data)	–
Litti et al. [83]	Aluminum NP via laser ablation synthesis in solution) + propynyl fluorescent red (PFR)	Erlotinib	0.3 μM	0.3 μM	3 \times diluted human plasma with trichloroacetic acid at 15%	633 nm, 8 mW, 785 nm, 10 mW	100 μl
Panikar et al. [84]	Hybrid SERS substrate based on graphene oxide (GO)-supported L-cysteine-functionalized star-like gold nanoparticles (SAUNPs)	Paclitaxel Cyclophosphamide	0.015 μM 0.005 μM	0.015 μM 0.005 μM	Undiluted serum	785 nm, 2.4 mW	10 μl
Sivashanmugan et al. [85]	Hybrid plasmonic-biosilica SERS substrate based on Ag NPs	Tetrahydrocannabinol	10 ⁻⁶ μM	–	Human plasma	532 nm (no power data)	1 ml
(D) In other body fluids							
Chen et al. [86]	Ag NP	Penicillin G residues	0.01 μM	2.54 nM	Milk	633 nm, 17 mW	4 ml
D'Elia et al. [87]	Au nanorods	Cocaine	0.03 μM	0.03 μM	Oral fluid	780 nm, 10 mW	5 μl
Kodama and Yamada [88]	Au nanorods	Sodium phenobarbital	1 mM	–	Tear	785 nm (portable), 30 mW	100 μl
Souza et al. [89]	Ag NPs/Agar films	Methamphetamine	10 μM	–	Fingerprints	633 nm, <1 mW	100 μl
Deriu et al. [90]	Au NP (spheres)	Cannabinoid JWH-018	0.11 μM	0.09 μM	Oral fluid – 37.5% v/v methanol	785 nm, 100 mW	400 μl
Sivashanmugan et al. [85]	Hybrid plasmonic-biosilica SERS substrate based on Ag NPs	Tetrahydrocannabinol	10 ⁻⁶ μM 0.001 μM	– –	Human plasma Raw saliva	532 nm (no power data)	1 ml

variations between different substrates of the same type would introduce unacceptable quantification errors. Currently, standard deviations of about 20% are still considered reasonable [72]. However, clinical and forensic applications must fulfill much higher standards and require significant improvements. Yan et al. [63] developed a method that ensures high reproducibility of gold (Au) nanoparticle (NP)-based SERS substrates. The technique is based on NPs transforming from the wet state to the dry state, forming optimal hot spots, arranged in a 3D long-range-ordered structure, which is stable for dozens of seconds [63]. The presented substrate provides good reproducibility; quantitative measurements showed a standard deviation of only 8.1% [63]. They tested the detection of the party drug 3,4-methylenedioxy-methamphetamine and the synthetic psychoactive drug α -methyltryptamine hydrochloride in water for concentrations down to 10 μM and 1 μM , respectively [63].

Besides gold, silver (Ag) is a frequently used metal for SERS substrates. Gao et al. presented Ag-Au-hybrid NPs with unusually long shelf life (12 months) [69] and strong binding of thiol groups, which is very useful for biomedical applications [69]. Ag NPs, in this case seeded on graphene nanosheets, have also proven to be sensitive for the anticancer drug 2-thiouracil down to 10 nm in water [67]. Haddad et al. [70] proposed an approach for monitoring the synthetic opioid fentanyl (also in mixture with heroin) using a simple paper-based substrate impregnated with Ag NPs [70]. Moreover, Hong et al. [91] developed Ag-nanogratings to monitor the antibiotics enofloxacin and ciprofloxacin, using a portable Raman spectrometer and chemometrics for quantification [91].

In addition to the noble metals, copper (Cu) was demonstrated to enable SERS. The Cu-NPs were temporally

protected against oxidation by porous calcium carbonate microspheres and enabled the sensitive detection of two antibacterial drugs (ceftriaxone and sulfadimethoxine) in injection solutions and tablets [72].

Also, colloidal Ag [68] and Au [66] NPs were useful for the detection of antibiotics [66, 68] and antimalarial active ingredients [68] in aqueous solutions and allowed quantification in pharmaceutical dosage forms such as (substandard) tablets [68] and eye drops [66]. However, in these cases either the preparation of the colloidal substrate [66] or the sample preparation [68] is quite time-consuming and extensive. An innovative strategy for TDM of the anti-cancer drug erlotinib using an Au-colloid-SERS assay was introduced by Litti et al. [83]. They used an internal reference – propynyl fluorescent red (PFR), a good Raman scatterer – which competes with the drug for the binding spots on the surface of functionalized gold NPs (see Figure 3). Usually, erlotinib levels are low and PFR dominantly binds to the surface of the Au NP clusters. The resulting intense PFR SERS signal is negatively proportional to the target drug concentration.

2.1.2 Towards SERS measurements in body fluids

Body fluids are challenging media for Raman sensing in general. The components of these liquids give rise to signals which can overlap with the signal from the substance of interest. Especially proteins complicate the measurement procedure, as they are fluorescent and thus cover the Raman signals of the analyte (e.g. drug). For SERS measurements, it should also be considered that proteins can bind the low-concentrated drugs or cover the

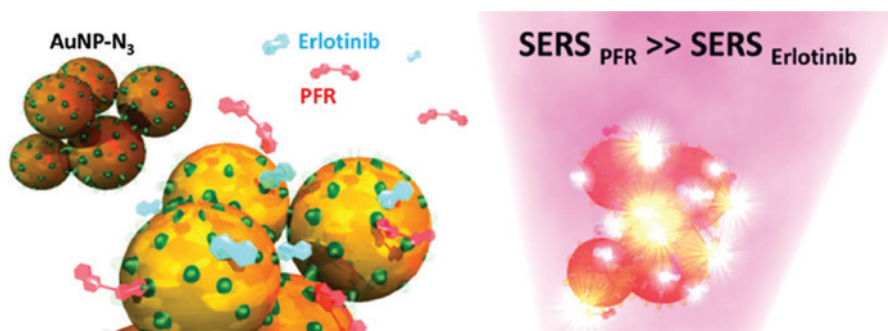


Figure 3: Schematic working principle of SERS mediated monitoring of the anti-cancer drug erlotinib.

Erlotinib and PFR compete for the azide-groups on the surface of the functionalized Au NP. In common applications, erlotinib levels are low and the strong Raman scatterer PFR dominates on the surface of the Au NP clusters. The resulting intense SERS signal is negatively proportional to the target drug concentration. Adapted from Litti et al. [83], reproduced with the kind permission of Elsevier, Copyright (2019) Elsevier.

NP surface of the SERS substrates, therefore inhibiting the activity of the “hot spots” [52].

Recently, special substrates were introduced to address the protein problem. Yue et al. [82] developed semipermeable alginate microparticles containing gold NPs [82]. The alginate membrane acts like a filter and only allows small molecules to enter and interact with the gold NPs. Large proteins are thus hindered from forming a protein corona around the Au NPs (Figure 4), resulting in a good SERS signal of the analyte [82]. In serum, this method could reach a reproducibility of 10% [82]. Panikar et al. introduced a brush layer to prevent SERS-hot spot blockages and fouling by blood serum proteins [84]. The monolayer is built by hierarchically modified, self-assembled zwitterionic L-cysteine [84]. The complete substrate is called graphene oxide (GO)-supported L-cysteine-functionalized star-like gold NPs (SAuNPs@GO) (Figure

5) [84]. It has additional advantages, such as a very high Raman signal enhancement factor as well as high stability and reproducibility [84]. Both approaches aim to find application in point-of-care TDM in cancer therapy [82, 84].

Another approach to overcome matrix-related challenges is to combine sample pretreatment methods with the sensing platform [73, 74, 76, 79, 81, 86, 88, 90]. For drug sensing in body fluids, several studies reported the combination of SERS and high-performance liquid chromatography (HPLC) [56]. Unfortunately, this combination compromises the advantage of Raman spectroscopy: quick and straightforward point-of-care applicability. Other reported separation techniques like liquid extraction [73, 74, 77], (ultra-)filtration [59, 79, 80, 88], and passing the sample through a purification column with silica gel [76] are more compatible with point-of-care use.

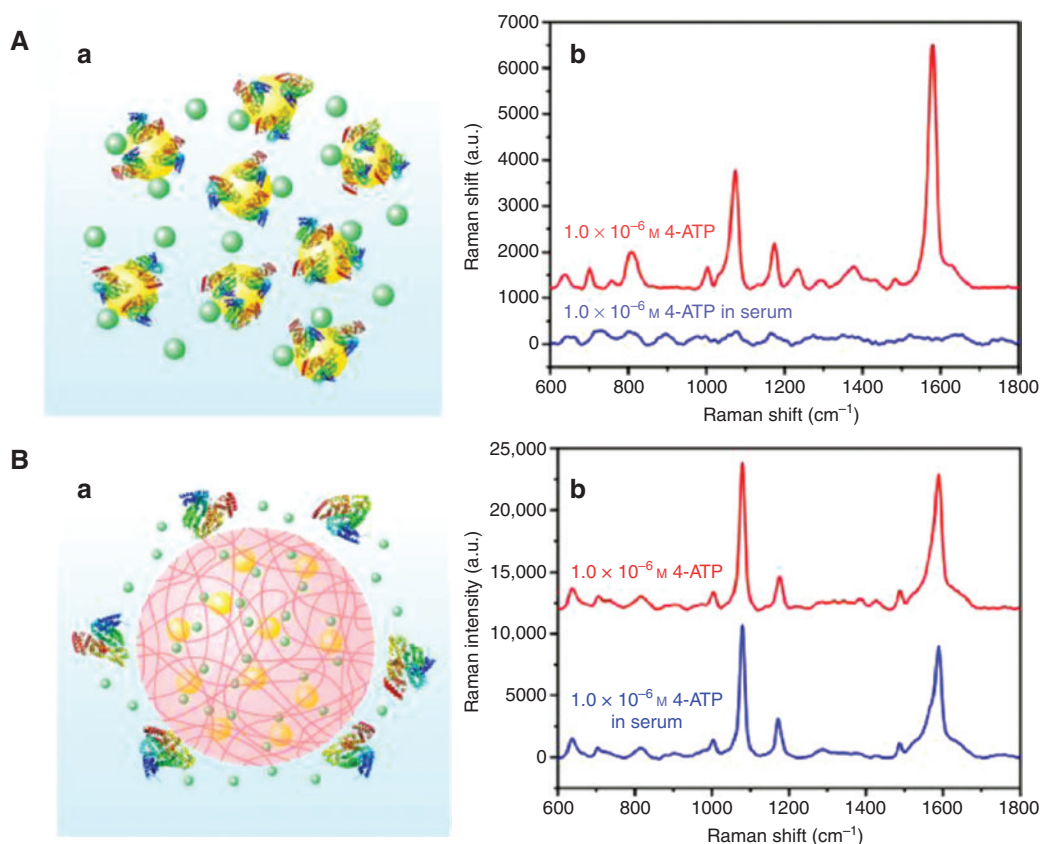


Figure 4: Depiction of the protein problem in SERS measurements and possible solutions.

(A, a) The nonspecific adsorption of proteins on Au NPs leads to “protein coronas” which block the analyte (e.g. drug) from entering the hot spots close to the NPs surface. (A, b) SERS measurements with colloidal gold: while the spectrum of 1.0×10^{-6} M 4-aminothiopheno (4-ATP) in aqueous solution (red) shows pronounced peaks, the spectrum for 1.0×10^{-6} M 4-ATP in serum (blue) has no characteristic features due to the protein problem. (B, a) Semipermeable microparticles prevent the diffusion of proteins but allow the diffusion of small molecules. The hot spots remain accessible, and the protein problem is avoided. (B, b) SERS measurements with colloidal gold within semipermeable microparticles: The spectra of 1.0×10^{-6} M 4-ATP in water and in serum both show strong characteristic features. Adapted from Yue et al. [82], reproduced with the kind permission of Elsevier, Copyright (2018) Elsevier.

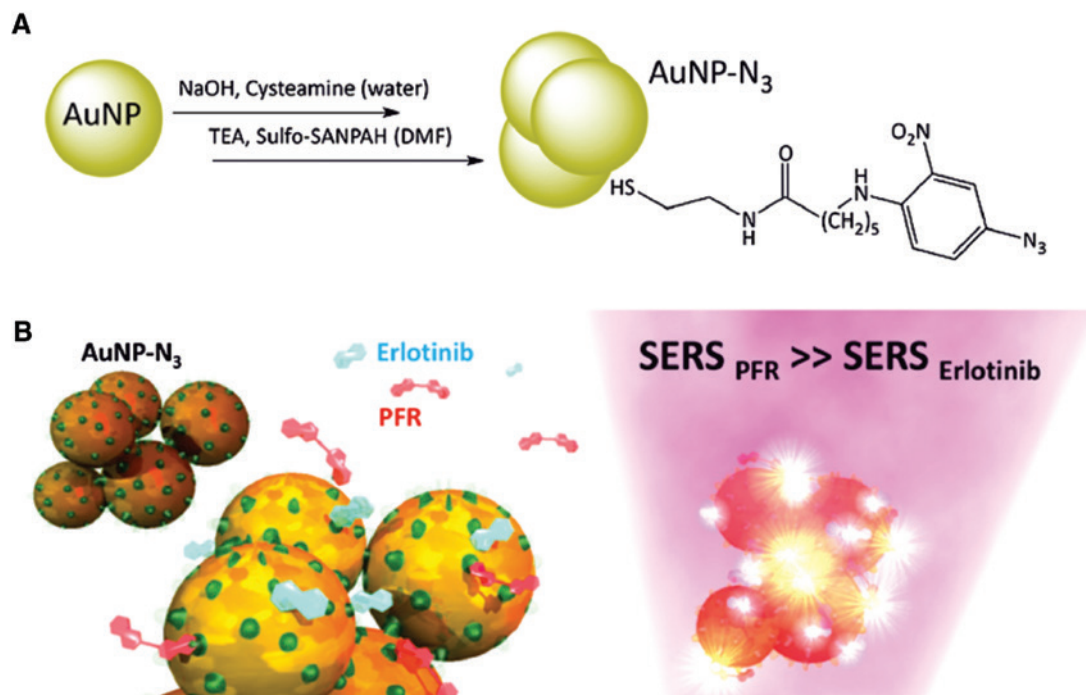


Figure 5: Schematic illustration of the production and application of a SERS substrate modified to avoid the protein problem. (A) Fabrication of the graphene oxide (GO)-supported functionalized starlike gold nanoparticles. L-cysteine is used to functionalize the NPs. (B) The L-cystein monolayer acts as brush layer and prevents blood serum proteins from blocking the SERS hot spots. Adapted from Panikar et al. [84], reproduced with the kind permission of the American Chemical Society, Copyright (2019) American Chemical Society.

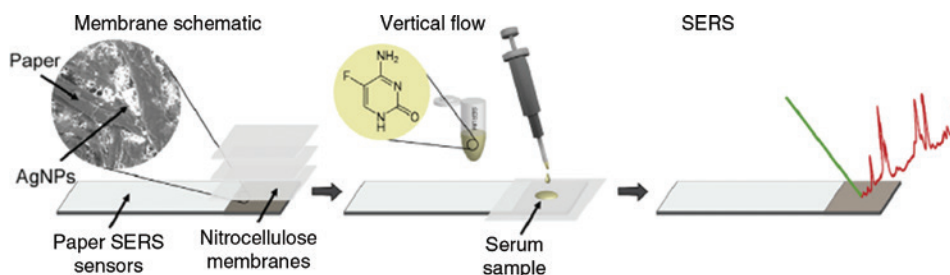


Figure 6: Working principle of a point-of-care applicable platform for SERS based on a paper-filtering membrane. The micro-structure is visible in the SEM picture of the Ag NPs on cellulose paper. After application of the sample liquid, proteins are separated from the active ingredients by vertical flow filtering. The SERS signal of the analytes can then be read from the paper SERS sensor. Adapted from Berger et al. [79], reproduced with the kind permission of Elsevier, Copyright (2017) Elsevier.

Berger et al. reported about a point-of-care applicable platform for SERS, based on a paper membrane for vertical flow separation [79]. The filter membrane is combined with inkjet-printed Ag NPs (Figure 6). This method has high potential as TDM tool in the clinic. The proposed procedure is simple; one measurement only takes 15 min overall, and the single components are cheap.

Besides blood, urine is another body fluid of interest. It is easily available without any invasive measures such as a needlestick. As a sample matrix, it is easier to handle because it does not contain as many proteins as serum or

plasma. Bindesri et al. [75] combined electrochemistry and SERS, using a fabric-based electrochemical plasmonic sensor [75]. All electrodes were impregnated with conducting silver ink, and the fabric was dried. An additional carbon ink line was deposited onto the working electrode and topped with Ag NP paste. The counter electrode was also coated with carbon ink, while the reference electrode remained unchanged (silver ink). When the sensor surface charges are manipulated through the application of voltage, neutral analyte species interact with the silver metal surface. Uncharged analytes can thus be measured

quickly and easily. In this study, the authors successfully tested their sensor for TDM of the antibiotic levofloxacin in synthetic urine down to a concentration of 1 mM [75].

Markina et al. [76] developed a fast detection method for another antibiotic (ceftriaxone) in urine, enabling SERS quantification in 10 min overall. The following simple pretreatment steps were used: pH adjustment, passing the sample through a purification column with silica gel, and filtering through a cellulose filter [76].

Urine is interesting not only for TDM applications, but also for forensic sensing, especially to determine drug abuse easily. Liquid-liquid microextraction is a common approach [73, 74, 77] for this purpose. This method can be quick as well; the overall process requires just 5–6 min [77].

2.2 Fiber-enhanced Raman spectroscopy for drug monitoring

Another very promising approach for high signal amplification with potential for on-site and point-of-care sensing was recently introduced with fiber-enhanced Raman spectroscopy (FERS) [47, 92–96]. In FERS, the laser light is coupled into a hollow-core optical fiber, which is also filled with the sample solution. The interaction between the guided laser light and the analyte molecules is thus increased over an extended length. As a result, the number of molecules interacting with the light is highly increased (Figure 7). For the fiber enhancement, several factors, such as laser intensity, fiber guiding properties and length, and the coupling efficiency play a major role [47]. These parameters differ

for different fiber types. For FERS sensing with hollow-core photonic crystal fibers (HC-PCFs), a tremendous increase in signal intensity is possible. Ten to fifty times higher sensitivities and improvements in limits of detection (LODs) of more than one order of magnitude have been achieved for pharmaceuticals dissolved in aqueous environment [97, 98]. FERS is a very flexible technique which can be miniaturized and shows high potential for point-of-care monitoring of drugs [97, 98] or biomarkers [99] (see Table 2).

The bandgap of specific HC-PCFs can be shifted into the visible range, when the fiber is filled with aqueous analyte solution (see Figure 8A). This effect was exploited for the monitoring of the antibiotic levofloxacin in the visible range (excitation wavelength 532 nm) down to a concentration of 20 μM [60]. The required sample volume for the filling of the sensor fiber is very low (8 nl). By selectively filling the central hollow core of the fiber [98], broadband step-index guiding is achieved. This enables the use of excitation wavelengths throughout the whole visible range (Figure 8B). Thus, the excitation wavelength can be chosen depending on the analyte requirements, taking spectral characteristics such as absorption maxima or fluorescence bands into account. In this way, additional enhancement can be achieved through the resonance Raman effect [99], and the spectral range where fluorescence is likely to occur might be avoided. Using a selectively filled fiber, a LOD of 1.7 μM was achieved for the antibiotic moxifloxacin in water [51].

FERS based on HC-PCFs was further exploited in combination with SERS [107]. Yet, it remains to be proven whether these approaches will be practicable for drug monitoring. So far, fiber-SERS techniques were only tested

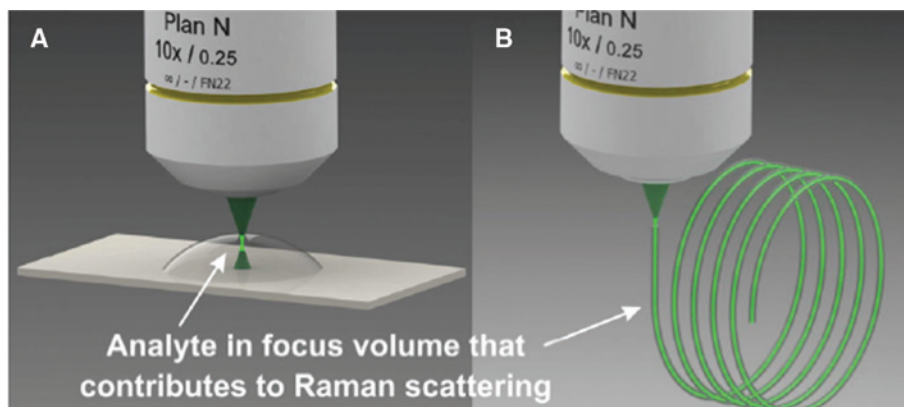
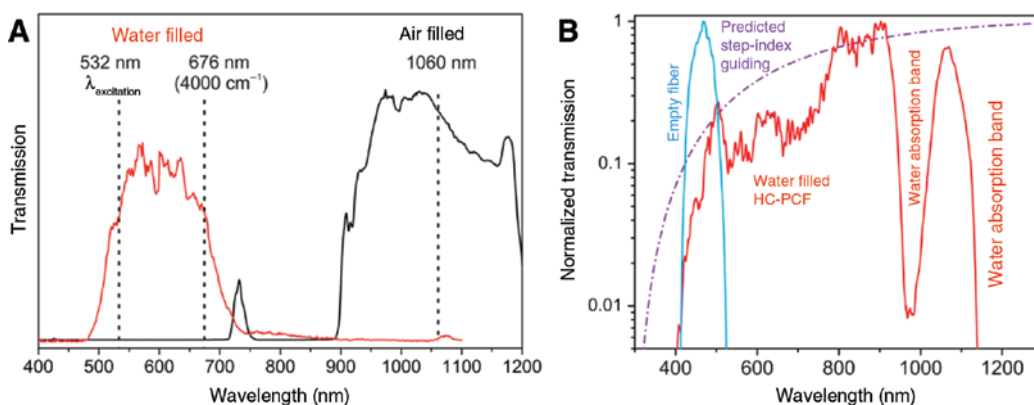


Figure 7: Comparison between the limited collection volume in conventional Raman spectroscopy (A) and the extended interaction volume in FERS (B).

Enhancement effect in FERS: The volume of interaction and light collection in conventional measurements (A) is limited to the focal volume. In FERS (B), the illuminating laser light is guided along the sample filled core of a fiber. The light-analyte interaction is thus increased and the Raman signal is enhanced. Adapted from Frosch et al. [47], reproduced with the kind permission of the American Chemical Society, Copyright (2013) American Chemical Society.

Table 2: Other Raman spectroscopic methods applied for pharmaceutical drug monitoring.

Reference	Drug	Lowest detected concentration	LOD	Medium	Excitation wavelength and laser power	Sample volume
(A) FERS						
Frosch et al. [47]	Chloroquine	75 μM	75 μM	Water	532 nm, 30 mW	38 μl
	Mefloquine	25 μM	25 μM			
	Chloroquine	0.2 μM	0.2 μM		257 nm, 2.4 mW	
	Mefloquine	0.06 μM	0.06 μM			
	Chloroquine	0.008 μM	0.008 μM		244 nm, 0.5 mW	
	Mefloquine	0.08 μM	0.08 μM			
Liu et al. [100]	Levofloxacin	–	–	Blood	633 nm, (no power data)	1 ml
Yan et al. [67]	Moxifloxacin	1.7 μM	1.7 μM	Water	532 nm, 100 mW	4 nl
Yan et al. [97]	Levofloxacin	20 μM	20 μM	Water	532 nm, 100 mW	8 nl
Yan et al. [101]	Cefuroxim	100 μM	100 μM	Urine	532 nm, 150 mW	104 nl
					785 nm, 350 mW	
Azkune et al. [102]	Glucose	5 mM	0.34 mM	Water	785 nm, 27.61 mW	1.33 μl
		1 M	–	Urine		
(B) Fiber-array based Raman imaging						
Frosch et al. [103]	Artemether	10% (w/w)	–	Tablet (hypromellose)	532 nm, 600 mW	–
	Lumefantrine	30% (w/w)	–			
(C) SORS						
Olds et al. [104]	Acetaminophen	5% (w/w)	–	Powder mixture (glucose and caffeine)	785 nm, 400 mW	–
	Phenylephrin	5% (w/w)	–			
Moody et al. [105]	Melatonin	100 μM	100 μM	Agarose gel behind cat bone	785 nm, 50 mW	200 μl
	Epinephrine					
	Serotonin					
Nicolson et al. [106]	Chalcogen-pyrylium dye 823	1 pM	104 fM	Porcine skin	830 nm, 450 mW	3 μl
	1,2-Bis(4-pyridyl) ethylene	11 pM	–			

**Figure 8:** Transmission spectra of two different hollow core fibers for FERS of liquids.

(A) Compared with the air-filled HC-PCF, the spectrum of the water filled fiber is blue-shifted into the visible spectral range. The sensor fiber is thus suited for FERS with a laser wavelength of 532 nm and Raman spectra up to 4000 cm^{-1} . (B) In this case, not the whole microstructure of the fiber is water filled. Instead, just the central core of the fiber is filled with water, leading to a change in guiding properties (from band-gap to step-index guidance). The measured spectrum roughly follows the prediction and shows that the fiber offers broadband transmission in the visible range. Adapted from Yan et al. [59, 97], reproduced with the kind permission of the Royal Society of Chemistry (A), Copyright (2017) Royal Society of Chemistry and the American Chemical Society (B), Copyright (2017) American Chemical Society.

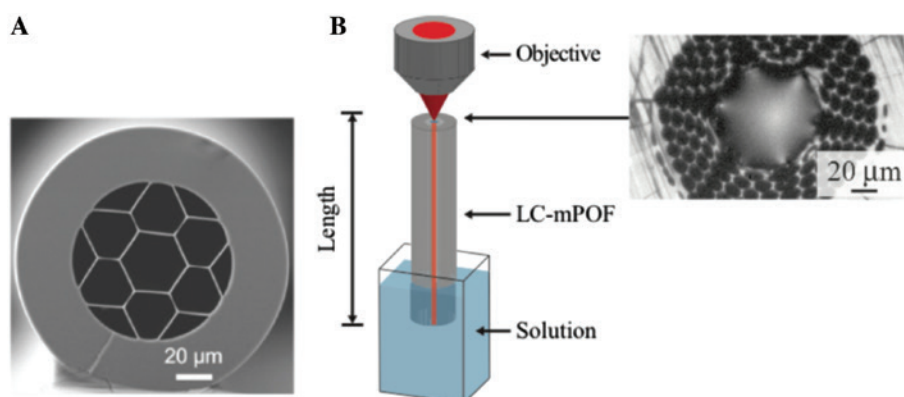


Figure 9: Cross sections of a novel silica air-clad hollow-core fiber (A) and polymer optical hollow-core fiber (B) for FERS sensing. (A) SEM image of the cross-section of an air-clad fiber which was developed specifically for highly sensitive drug monitoring. The diameter of the central core is approximately $30\ \mu\text{m}$. (B) Experimental setup for FERS for glucose sensing. The microstructure of the polymer hollow-core optical fiber is modified on one end: all openings but the central core are closed. This end is dipped into the sample solution which is sucked into the central core as a result of the capillary effect. Laser coupling and signal collection through an objective lens takes place at the other end of the fiber. The inset shows a microscope image of the upper end face of the micro-structured polymer hollow-core optical fiber. Adapted from Yan et al. [107] (A) and from Azkune et al. [102] (B), reproduced with the kind permission of the American Chemical Society, Copyright (2018) American Chemical Society (A) and IEEE (B).

for the detection of model substances, biomarkers, or cells for biomedical applications but not yet for approved pharmaceuticals [107].

There is a major drawback using HC-PCFs. The small central hollow core is difficult to fill with analyte solutions and also hampers stable light coupling. To efficiently integrate the fiber into a spectroscopic system, the coupling needs to be very precise. To achieve 90% performance, a lateral offset of just $\pm 1.5\ \mu\text{m}$ is allowed [97].

This challenge can be solved by using customized air-clad fibers (Figure 9A) with bigger central core, which were specifically tailored for highly sensitive drug monitoring [101]. FERS with these fibers enabled a signal enhancement factor of about 60 times for the antibiotic cefuroxime [101]. The broadband guiding mechanism of this selectively filled fiber type allows the use of different excitation wavelengths in the visible and also up to the near infrared (NIR) range. By choosing the excitation wavelength of 835 nm, fluorescence background of human urine could be avoided [101]. Drug monitoring in human urine was possible down to concentrations of $100\ \mu\text{M}$ [101]. Moreover, the method was validated on real urine samples from volunteers and cross referenced with HPLC measurements. Thus, this approach proves to be a very promising alternative to the time-consuming, lab-based TDM methods used up to date.

Recently, Azkune et al. reported about a micro-structured polymer hollow-core optical fiber (POF) system (Figure 9B) that was used for glucose sensing [102]. This FERS platform could perspective be used for TDM of the sodium-glucose co-transporter 2 inhibitors in the therapy of diabetes mellitus. Through careful preparation of the fiber and additional

steps in data processing and analysis, glucose sensing in urine could be demonstrated via POF-FERS [102].

2.3 Fiber-array based Raman chemical imaging for drug monitoring

In pharmaceutical applications, it would be ideal to gain complete qualitative and quantitative information about the chemical composition of a formulation preferably in a short time. The distribution and the particle size of the APIs strongly influence the biopharmaceutical profile of the formulations. Yet, these properties are neither directly analyzed during the production process nor in the formulation. For the quality assuring analysis of the active ingredients' concentrations and their pharmacokinetic profile, the samples have to be dissolved. This is time consuming, and the analysis requires expensive instrumentation. This aspect is especially critical in the case of counterfeit medicines, which are spreading all over the world, and in a greater extent in poor countries.

To address this problem, a fiber-array-based chemical imaging method [103, 108, 109] was adapted and successfully applied for counterfeit and substandard tests of the antimalarial tablet Riamet® [103]. This technique exploits the flexibility and efficiency of light guidance in optical fibers and enables the readout of numerous spectra from different regions of the sample [103, 108, 109] (see Figure 10). Therefore, chemical imaging of a large area is possible with high spatial resolution. In the antimalarial tablets, the two active ingredients artemether

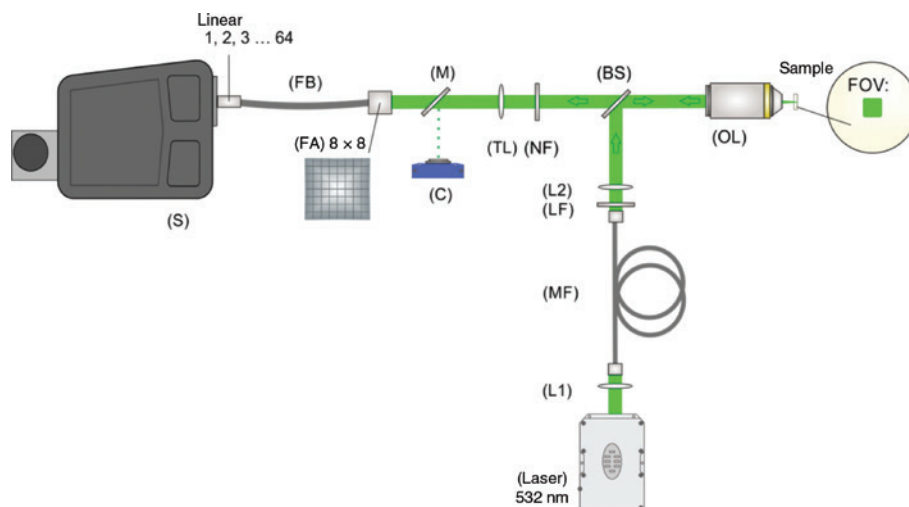


Figure 10: Sketch of the experimental setup for fiber array-based Raman hyperspectral imaging.

The rectangular area of illumination in the focal plane is achieved with a long propagation length of the laser light within a step index multimode fiber (MF). The backscattered signal is imaged onto an 8×8 fiber array. The fiber arrangement within the fiber bundle (FB) changes from 8×8 square to 64×1 line. The linear array is positioned in the slit plane of the spectrometer enabling hyperspectral imaging with reduced effort for acquisition. Adapted from Frosch et al. [103], reproduced with the kind permission of MDPI.

and lumefantrine were quantified simultaneously *in situ*, without dissolution. With this setup, the distribution of active ingredients can be visualized in a time efficient way, as in one shot 64 regions can be imaged with a spatial resolution of about $1 \mu\text{m}$ [103]. Consequently, fiber-array based Raman imaging has a high potential to become an on-line or at-line quality control method for pharmaceuticals.

Furthermore, fiber-array based Raman imaging could help to speed up SERS measurements. In SERS, a lot of spectra are needed for robust quantitative measurements (e.g. in the study of Souza et al. [89] at least 100 spectra are required). Frequently, the sample surface is mapped for this reason. However, the time-consuming mapping is limiting the measurement speed [110] which could be mitigated using an array-based imaging approach [103].

2.4 Spatially offset Raman spectroscopy for drug monitoring

Spatially offset Raman spectroscopy (SORS) allows the detection of analytes below a non-absorbing cover material, such as in the case of packaged pharmaceuticals [111]. This is realized by the acquisition of two Raman spectra: first from the container, in conventional geometry, and second from a deeper layer by lateral offset from the illumination spot. The principle is the following (Figure 11): as the incident laser light reaches the sample, part of the light will reach deeper layers of the sample (with exponentially decaying intensity). Equally, some of the diffuse

Raman-scattered photons will migrate upwards with a lateral offset. [112] The second Raman spectrum recorded with the lateral offset is then scaled and subtracted from the first, yielding the subsurface Raman spectrum [111]. The deeper the layer of interest, the larger is the necessary spatial offset of the detection.

Using this method in combination with multivariate analysis, several pharmaceuticals were detected [111] and quantified [104]. Olds et al. [104] reported about the quantification of the frequently used analgesic acetaminophen (also called paracetamol) and the decongestant agent phenylephrine in a powder mixture with glucose and caffeine down to 5% [104] through the polypropylene container. Zhang et al. [113] reported the detection of acetaminophen and the antibiotic drug metronidazole through polyethylene and polytetrafluoroethylene bottles [113].

The SORS technique was advanced and developed into a handheld device called “Resolve” by the company Cobalt Light Systems Ltd (part of Agilent Technologies). The method can thus be applied in the field, e.g. for the detection of toxic industrial chemicals, flammable compounds, explosives, narcotics, and chemical warfare agents [114].

The sensitivity and specificity of this technique can be further increased by combining SORS with SERS: the so called SESORS [115, 116]. Stone et al. reported about resonant SERS-active molecule-specific reporter NP conjugates, which can be delivered into the skin and provide disease-specific Raman signatures [77]. Resonant dyes as conjugants enable the detection of very low reporter molecule concentrations, as the dyes deliver highly enhanced

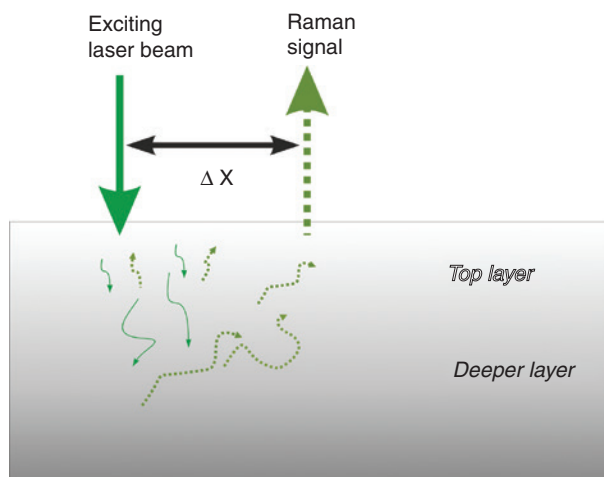


Figure 11: Principle of spatially offset Raman spectroscopy. Raman scattered light from deeper layers can be collected at a distance Δx from the spot of illumination. The larger the distance, the higher the ratio of signal from deeper layers, but also the smaller the signal intensity. $\Delta x = 0$ is equal to the signal collection geometry of conventional Raman spectroscopy.

signals. These Raman signals can be recorded with the help of the deep Raman technique SORS through thick tissues of several tens of millimeters [116], pushing the LODs far beyond conventional SORS [116]. This method might find further application in monitoring drugs or drug delivery processes in different tissues.

The first step in this direction was already taken by Moody et al. They analyzed neurotransmitters in brain-mimicking agarose gel through a cat skull via SESORS [105]. Combining this method with principal component analysis, the authors could differentiate between the neurotransmitters melatonin, serotonin, and epinephrine [105].

Combining SORS with Raman imaging for the detection of explosives from a distance [117] allows the collection of information from different spatial offsets simultaneously. Thus, the imaging facilitates the process, as the optimal spatial offset is unknown [117]. Overall, SORS is a very promising method for applications in pharmaceutical, forensic, and security substance monitoring and enables tests through the packaging.

2.5 Raman optical activity and enantioselective Raman spectroscopy for drug monitoring

Many pharmaceutical drugs and biomolecules are chiral substances. These molecules can exist in at least two different

steric formations, i.e. left-handed (l) or right-handed (d). The two versions are called enantiomers. The stereo-chemical structure of a pharmaceutical active ingredient is decisive for the binding to its specific target structure (often proteins or DNA). Enantioselective Raman spectroscopy (EsR) and Raman optical activity (ROA) are specific Raman techniques for the identification and quantification of chiral molecules. Both techniques take advantage of the optical activity of chiral molecules. Optical activity describes the phenomenon that the interaction of polarized light with left-handed or right-handed enantiomers leads to different effects.

EsR is a novel approach developed by Kiefer et al. [118] based on polarization resolved signal detection. The sample is illuminated with linearly polarized laser light, and a half-wave retarder in the detection arm of the setup enables the investigation of the optical activity of the sample. As a result, enantiomers can be distinguished and enantiomeric fractions can be determined [119]. EsR is thus promising, e.g. for the on-line monitoring of synthesis processes of chiral drugs [120]. The approach was recently advanced with an automatized polarization-resolved Raman setup and coupled with chemometric analysis [119, 121] which enabled enantiomeric differentiation of butan-2-ol [120, 121]. Also, the enantiomeric fractions of the chiral molecule (5,6)-diphenyl-morpholin-2-one could be determined [119].

ROA takes advantage of the fact that excitation of the sample by right- or left-circularly polarized light results in differences in the Raman spectra [122]. Employing this approach, Gašior-Głogowska et al. [123] monitored the interaction of the anticancer drug cisplatin with the target DNA structure via the detection of conformational rearrangements within the chiral sugar moieties [123].

EsR and ROA could be especially interesting for the *in situ* quality assessment of novel biopharmaceuticals, particularly where glycoproteins play a pivotal role [124]. They could help to characterize the polypeptide backbone and the carbohydrate conformation at the same time. In the first study about the application of ROA for the investigation of a biopharmaceutical formulation, a therapeutic monoclonal antibody was characterized, looking into detail at the overall three-dimensional structure of the protein [125].

The implementation of these techniques in drug sensing is still very limited. EsR is just emerging, the nearest to real drug application was the reported proof-of-principle study with a morpholinone derivative [119].

The major challenge for the application of ROA is the extremely low signal intensity, which is three to five orders of magnitude lower than in conventional Raman scattering [126]. Therefore, enhancement techniques are necessary. Analog to other Raman techniques, ROA can be combined

with SERS, exploiting the enhancement effect of surface plasmon resonance. Surface-enhanced Raman optical activity (SEROA) was tested using Ag nanowires for the detection of the peptide fmoc-glycyl-glycine-OH [126]. Furthermore, a special nanotag was developed for analyzing d- and l-tryptophan and d- and l-ribose. The nanotag is based on a Ag NP core coated in a silica shell, to which the benzotriazole reporter molecule and the analyte are attached [127]. Recently, another approach for SEROA has been published by Wu et al. [128]. Here, the authors used hybrid magnetic NPs and showed that the ROA to Raman ratio is enhanced by the magnetic properties of the NPs [128].

It is not known yet how these advanced ROA approaches will perform in investigations of structural and thus qualitative changes of real biopharmaceuticals. Nevertheless, the developments in this direction are promising for the sensitive detection of peptide and sugar structures and their moieties upon drug action or degradation processes.

3 Prospects and challenges for Raman spectroscopic techniques for drug monitoring

3.1 Drug monitoring in the development of pharmaceuticals

In pharmaceuticals, chemically selective methods are highly desired as PAT for on-line or in-line quality control. Raman spectroscopic techniques could meet the requirements. Currently available portable Raman spectrometers facilitate the application in the pharmaceutical industry [14], but their low sensitivity and spectral resolution limit the use. However, continuous improvements and newly developed technologies are expanding the range of applications.

Fiber-based systems can be used at-line or in-line and allow high flexibility. Especially for chemical imaging, fiber-based techniques are very promising. APIs in solid dosage forms can be monitored without dissolution. Data acquisition speed can be improved markedly while high spatial resolution is maintained [103].

Going deeper, subsurface Raman techniques, such as SORS, provide a solution for the measurement of the drug content through the package [104, 111]. The low signal intensities can be significantly enhanced by combining SORS with SERS (SESORS). However, the applicability of SORS is limited when the sample is highly absorbing at

the laser or Raman signal wavelengths. Absorption greatly reduces photon propagation distances and penetration depths [115]. Raman signals from deeper layers require larger spatial offset detection which results in lower signal intensities from the target. Consequently, penetration depth and needed signal intensity have to be balanced.

For *in situ* quality assessment of biopharmaceuticals, advanced ROA methods, such as SEROA, are highly interesting. However, due to the very low intensity of ROA (even with plasmonic resonance enhancement), the technique requires higher sample concentrations and longer data collection periods. This can induce adverse laser light-derived degradations of sensitive APIs. FERS could be an option for further enhancement [47, 92].

Furthermore, FERS could also be exploited for monitoring dissolution processes in low sample volumes in a highly sensitive and chemically selective way. Both flow-through and static chambers could be realized for FERS. To advance FERS towards these applications, further developments in instrumentation are needed to ensure good sensitivity, reproducibility, and easy handling.

All Raman techniques still face difficulties with fluorescent samples. This problem can be balanced by adapting the excitation wavelength to the sample characteristics. In the visible range, spectral windows are very specific for each analyte and matrix. Choosing one wavelength would thus restrict the universal use of a device. To avoid fluorescence signals in general, both NIR and deep-UV light could be used for typical samples in drug monitoring. However, both wavelength ranges have their specific challenges. The Raman scattering effect is intrinsically weaker in the NIR range, leading to unfavorably low signal intensities. For UV, a significant signal enhancement can be achieved, but currently available optical components for the deep-UV range are not as efficient as in the visible range.

Elaborate data processing methods are needed in all Raman spectroscopic applications in the field of pharmaceuticals. This is especially true when complex mixtures are investigated. Multivariate data analysis is often applied [129]. Advances in chemometrics and data-driven classification approaches will lead to automation and easy interpretation of results.

3.2 TDM and forensic sensing

Methods for fast on-site, highly selective, and ultra-sensitive drug sensing are sought after for clinical and forensic applications. TDM of anticancer agents and antibiotics improves the outcome of the patients. Yet, the long

sample-to-result times of standard techniques hinder swift dose adaptations. Therefore, new methods are essential to achieve continuous and real-time drug monitoring at the point of care. Raman spectroscopic techniques are chemically selective and fast and can be miniaturized and applied at the point of care. However, the sensitivities required for the above-mentioned applications are challenging for conventional Raman sensing. Several enhancement strategies were successfully developed and advanced to meet this challenge.

In SERS, various advances were achieved for TDM [52, 75, 76, 79, 81, 83, 84, 97] of antibiotics [41, 75] and anti-cancer drugs [32, 35, 38, 81, 130]. Innovative SERS substrates [82, 84] represent a breakthrough towards clinical application as they overcome difficulties related to proteins in body fluids. Several approaches combine sample pretreatment methods with SERS detection [73, 74, 76, 79, 81, 86, 88, 90]. Some of the reported separation techniques result in extensive sample-to-result times (e.g. with 45 min [81] or more than 1 h [88]). These methods are not suitable for near-real-time drug monitoring. Other methods based on liquid extraction [77], filtration [59, 79, 80, 88], or purification columns [76] can be applied easily within 5 [77] to 15 min [79]. These preprocessing methods are compatible with future point-of-care use and could be automatized and included in a measurement procedure.

Complex nanophotonic technologies also show potential for the tracing of illegal or adulterant drugs [73, 74, 85, 87, 89, 131–135]. With the developed techniques, drugs can even be traced in fingerprints [89] or in body fluids other than blood or urine such as saliva [87, 90, 136]. D'Elia et al. recently reported about the extremely sensitive detection of cocaine in saliva via SERS, without any sample preparation [47].

There are two remaining major drawbacks that keep SERS away from widespread application: on the one hand, the complicated procedure for the synthesis of sophisticated plasmonic substrates and, on the other hand, the low reproducibility of SERS measurements (relative standard deviations about 20% are considered reasonable [72]). However, recent developments are promising. Novel substrates with shelf lives of up to 12 months [69, 72, 89] guarantee short-notice availability. Other materials achieved high reproducibility [77, 78] and low relative standard deviations (around 5% [71]). These results show that clinical or forensic standards are within reach of SERS methods.

FERS is another very promising Raman technique for continuous drug monitoring. Recent advances demonstrate the potential of FERS for TDM of antibiotics [97, 98, 101]. Different types of micro- and nano-structured sensor fibers, such as HC-PCFs [97, 98] and airclad fibers [101, 102], are developed, and their potential for clinical

applications is explored. The first step towards clinical application was recently taken, as a selectively filled airclad fiber was used for the monitoring of the antibiotic cefuroxime in human urine [101].

The reviewed scientific reports demonstrate that Raman spectroscopic techniques greatly advanced in recent years. Several promising techniques for pharmaceutical drug monitoring take advantage of new nano-phonic developments, such as improved SERS substrates and tailor-made micro- and nano-structured optical fibers. Expected improvements and further steps – like the combination of different Raman techniques – will open up new fields of application, i.e. on-site or point-of-care drug monitoring in body fluids.

Acknowledgment: Funding from the Deutsche Forschungsgemeinschaft (DFG: CRC 1076 AquaDiva) is gratefully acknowledged. The publication of this article was funded by the Open Access Fund of the Leibniz Association.

References

- [1] WHO. The top 10 causes of death. Available at: <https://www.who.int/news-room/fact-sheets/detail/the-top-10-causes-of-death>. Accessed: 30 Sep 2019.
- [2] Gary HL. Impact of chemotherapy dose intensity on cancer patient outcomes. *J Natl Compr Canc Netw* 2009;7:99–108.
- [3] Rebollo J, Valenzuela B, Duart-Duart M, Escudero-Ortiz V, Gonzalez MS, Brugarolas A. Use of therapeutic drug monitoring of cancer chemotherapy to modify initial per-protocol doses. *J Clin Oncol* 2010;28:e13015.
- [4] Bach DM, Straseski JA, Clarke W. Therapeutic drug monitoring in cancer chemotherapy. *Bioanalysis* 2010;2:863–79.
- [5] Sakr Y, Jaschinski U, Wittebole X, et al. Sepsis in intensive care unit patients: worldwide data from the intensive care over nations audit. *Open Forum Infect Dis* 2018;5:ofy313.
- [6] Vincent JL, Sakr Y, Sprung CL, et al. Sepsis in European intensive care units: results of the SOAP study. *Crit Care Med* 2006;34:344–53.
- [7] Roberts DM, Roberts JA, Roberts MS, et al. Variability of antibiotic concentrations in critically ill patients receiving continuous renal replacement therapy: a multicentre pharmacokinetic study. *Crit Care Med* 2012;40:1523–8.
- [8] Taccone FS, Laterre PF, Dugernier T, et al. Insufficient β -lactam concentrations in the early phase of severe sepsis and septic shock. *Crit Care* 2010;14:R126.
- [9] Robertson JL, Senger R. System and method using Raman spectroscopy for monitoring the health of hemodialysis and peritoneal dialysis patients. WO2015164620A1, 2015.
- [10] Roberts JA, Norris R, Paterson DL, Martin JH. Therapeutic drug monitoring of antimicrobials. *Brit J Clin Pharmacol* 2012;73:27–36.
- [11] Wong G, Briscoe S, McWhinney B, et al. Therapeutic drug monitoring of beta-lactam antibiotics in the critically ill: direct measurement of unbound drug concentrations to

- achieve appropriate drug exposures. *J Antimicrob Chemother* 2018;73:3087–94.
- [12] Nosseir NS, Michels G, Pfister R, Adam R, Wiesen MH, Müller C. [Therapeutic drug monitoring of anti-infectives in intensive care medicine]. *Deut Med Wochenschr* 2014;139:1889–94.
- [13] Singh R, Sahay A, Muzzio F, Ilerapetritou M, Ramachandran R. A systematic framework for onsite design and implementation of a control system in a continuous tablet manufacturing process. *Comput Chem Eng* 2014;66:186–200.
- [14] Jiménez-González C, Poechlauer P, Broxterman QB, et al. Key green engineering research areas for sustainable manufacturing: a perspective from pharmaceutical and fine chemicals manufacturers. *Org Process Res Dev* 2011;15:900–11.
- [15] Hinz DC. Process analytical technologies in the pharmaceutical industry: the FDA's PAT initiative. *Anal Bioanal Chem* 2006;384:1036–42.
- [16] Long DA. The Raman effect: a unified treatment of the theory of Raman scattering by molecules. John Wiley & Sons, Inc., 2002.
- [17] Knebl A, Yan D, Popp J, Frosch T. Fiber enhanced Raman gas spectroscopy. *TrAC Trends Anal Chem* 2018;103:230–8.
- [18] Frosch T, Popp J. Structural analysis of the antimalarial drug halofantrine by means of Raman spectroscopy and density functional theory calculations. *J Biomed Opt* 2010;15:041516.
- [19] Sieburg A, Schneider S, Yan D, Popp J, Frosch T. Monitoring of gas composition in a laboratory biogas plant using cavity enhanced Raman spectroscopy. *Analyst* 2018;143:1358–66.
- [20] Keiner R, Herrmann M, Kusel K, Popp J, Frosch T. Rapid monitoring of intermediate states and mass balance of nitrogen during denitrification by means of cavity enhanced Raman multi-gas sensing. *Anal Chim Acta* 2015;864:39–47.
- [21] Jochum T, Michalzik B, Bachmann A, Popp J, Frosch T. Microbial respiration and natural attenuation of benzene contaminated soils investigated by cavity enhanced Raman multi-gas spectroscopy. *Analyst* 2015;140:3143–9.
- [22] Hanf S, Bogozí T, Keiner R, Frosch T, Popp J. Fast and highly sensitive fiber-enhanced Raman spectroscopic monitoring of molecular H₂ and CH₄ for point-of-care diagnosis of malabsorption disorders in exhaled human breath. *Anal Chem* 2015;87:982–8.
- [23] Bogozí T, Popp J, Frosch T. Fiber-enhanced Raman multi-gas spectroscopy: what is the potential of its application to breath analysis? *Bioanalysis* 2015;7:281–4.
- [24] Sieburg A, Jochum T, Trumbore SE, Popp J, Frosch T. Onsite cavity enhanced Raman spectrometry for the investigation of gas exchange processes in the Earth's critical zone. *Analyst* 2017;142:3360–9.
- [25] Jochum T, Fastnacht A, Trumbore SE, Popp J, Frosch T. Direct Raman spectroscopic measurements of biological nitrogen fixation under natural conditions: an analytical approach for studying nitrogenase activity. *Anal Chem* 2017;89:1117–22.
- [26] Jochum T, von Fischer JC, Trumbore S, Popp J, Frosch T. Multigas leakage correction in static environmental chambers using sulfur hexafluoride and Raman spectroscopy. *Anal Chem* 2015;87:11137–42.
- [27] Hanf S, Fischer S, Hartmann H, et al. Online investigation of respiratory quotients in *Pinus sylvestris* and *Picea abies* during drought and shading by means of cavity-enhanced Raman multi-gas spectrometry. *Analyst* 2015;140:4473–81.
- [28] Bourgeois JP, Vorlet O. Low-cost portable Raman instrument, a tool toward counterfeit medication identification. *Chimia* 2018;72:905–6.
- [29] Gerace E, Seganti F, Luciano C, et al. On-site identification of psychoactive drugs by portable Raman spectroscopy during drug-checking service in electronic music events. *Drug Alcohol Rev* 2019;38:50–6.
- [30] Li JW, Cai F, Dong Y, et al. A portable confocal hyperspectral microscope without any scan or tube lens and its application in fluorescence and Raman spectral imaging. *Opt Commun* 2017;392:1–6.
- [31] Tondepu C, Toth R, Navin CV, Lawson LS, Rodriguez JD. Screening of unapproved drugs using portable Raman spectroscopy. *Anal Chim Acta* 2017;973:75–81.
- [32] Deidda R, Sacre P-Y, Clavaud M, et al. Vibrational spectroscopy in analysis of pharmaceuticals: critical review of innovative portable and handheld NIR and Raman spectrophotometers. *Trac-Trends Anal Chem* 2019;114:251–9.
- [33] Frosch T, Schmitt M, Popp J. Raman spectroscopic investigation of the antimalarial agent mefloquine. *Anal Bioanal Chem* 2007;387:1749–57.
- [34] Frosch T, Schmitt M, Noll T, Bringmann G, Schenzel K, Popp J. Ultrasensitive in situ tracing of the alkaloid dioncophylline A in the tropical liana *Triphyophyllum peltatum* by applying deep-UV resonance Raman microscopy. *Anal Chem* 2007;79:986–93.
- [35] Frosch T, Schmitt M, Schenzel K, et al. In vivo localization and identification of the antiplasmodial alkaloid dioncophylline A in the tropical liana *Triphyophyllum peltatum* by a combination of fluorescence, near infrared Fourier transform Raman microscopy, and density functional theory calculations. *Biopolymers* 2006;82:295–300.
- [36] Domes R, Domes C, Albert CR, Bringmann G, Popp J, Frosch T. Vibrational spectroscopic characterization of arylisoquinolines by means of Raman spectroscopy and density functional theory calculations. *Phys Chem Chem Phys* 2017;19:29918–26.
- [37] Domes C, Domes R, Popp J, Pletz MW, Frosch T. Ultrasensitive detection of antiseptic antibiotics in aqueous media and human urine using deep UV resonance Raman spectroscopy. *Anal Chem (Washington, DC, U. S.)* 2017;89:9997–10003.
- [38] Frosch T, Meyer T, Schmitt M, Popp J. Device for Raman difference spectroscopy. *Anal Chem* 2007;79:6159–66.
- [39] Frosch T, Schmitt M, Bringmann G, Kiefer W, Popp J. Structural analysis of the anti-malaria active agent chloroquine under physiological conditions. *J Phys Chem B* 2007;111:1815–22.
- [40] de Araujo WR, Cardoso TMG, da Rocha RG, et al. Portable analytical platforms for forensic chemistry: a review. *Anal Chim Acta* 2018;1034:1–21.
- [41] Matousek P, Parker AW. Bulk Raman analysis of pharmaceutical tablets. *Appl Spectrosc* 2006;60:1353–7.
- [42] Inoue M, Hisada H, Koide T, et al. Transmission low-frequency Raman spectroscopy for quantification of crystalline polymorphs in pharmaceutical tablets. *Anal Chem* 2019;91:1997–2003.
- [43] Terada H, Hattori Y, Sasaki T, Otsuka M. Quantitation of trace amorphous solifenacin succinate in pharmaceutical formulations by transmission Raman spectroscopy. *Int J Pharm* 2019;565:325–32.
- [44] Griffen JA, Owen AW, Matousek P. Quantifying low levels (<0.5% w/w) of warfarin sodium salts in oral solid dose forms using transmission Raman spectroscopy. *J Pharm Biomed Anal* 2018;155:276–83.

- [45] Villaumié J, Jeffreys H. Revolutionising Raman with the transmission technique. *Eur Pharm Rev* 2015;20:41–5.
- [46] Andrews D, Geentjens K, Igne B. Analytical method development using transmission Raman spectroscopy for pharmaceutical assays and compliance with regulatory guidelines—Part I: transmission Raman spectroscopy and method development. *J Pharm Innov* 2018;13:121–32.
- [47] Frosch T, Yan D, Popp J. Ultrasensitive fiber enhanced UV resonance Raman sensing of drugs. *Anal Chem* (Washington, DC, U. S.) 2013;85:6264–71.
- [48] Jeanmaire DL, Van Duynne RP. Surface Raman spectroelectrochemistry: Part I. Heterocyclic, aromatic, and aliphatic amines adsorbed on the anodized silver electrode. *J Electroanal Chem Interf Electr* 1977;84:1–20.
- [49] Albrecht MG, Creighton JA. Anomalous intense Raman spectra of pyridine at a silver electrode. *J Am Chem Soc* 1977;99:5215–7.
- [50] Fleischmann M, Hendra PJ, McQuillan AJ. Raman spectra of pyridine adsorbed at a silver electrode. *Chem Phys Lett* 1974;26:163–6.
- [51] Le Ru EC, Etchegoin PG. Principles of surface-enhanced Raman spectroscopy. Amsterdam, Netherlands, Elsevier, 2009:185–264.
- [52] Jaworska A, Fornasaro S, Sergo V, Bonifacio A. Potential of surface enhanced Raman spectroscopy (SERS) in therapeutic drug monitoring (TDM). A critical review. *Biosensors* (Basel) 2016;6:E47.
- [53] Lee PC, Meisel D. Adsorption and surface-enhanced Raman of dyes on silver and gold sols. *J Phys Chem* 1982;86:3391–5.
- [54] Buckley K, Ryder AG. Applications of Raman spectroscopy in biopharmaceutical manufacturing: a short review. *Appl Spectrosc* 2017;71:1085–116.
- [55] Cailletaud J, De Bleye C, Dumont E, et al. Critical review of surface-enhanced Raman spectroscopy applications in the pharmaceutical field. *J Pharmaceut Biomed* 2018;147:458–72.
- [56] Alula MT, Mengesha ZT, Mwenesongole E. Advances in surface-enhanced Raman spectroscopy for analysis of pharmaceuticals: a review. *Vib* 2018;98:50–63.
- [57] McAughtrie S, Faulds K, Graham D. Surface enhanced Raman spectroscopy (SERS): potential applications for disease detection and treatment. *J Photochem Photobiol* 2014;21:40–53.
- [58] Cialla-May D, Zheng XS, Weber K, Popp J. Recent progress in surface-enhanced Raman spectroscopy for biological and biomedical applications: from cells to clinics. *Chem Soc Rev* 2017;46:3945–61.
- [59] Jahn I, Žukovskaja O, Zheng XS, et al. Surface-enhanced Raman spectroscopy and microfluidic platforms: challenges, solutions and potential applications. *Analyst* 2017;142:1022–47.
- [60] Zong C, Xu M, Xu LJ, et al. Surface-enhanced Raman spectroscopy for bioanalysis: reliability and challenges. *Chem Rev* 2018;118:4946–80.
- [61] Chisanga M, Muhamadali H, Ellis D, Goodacre R. Enhancing disease diagnosis: biomedical applications of surface-enhanced Raman scattering. *Appl Sci* 2019;9:1163.
- [62] Khandasamy SR, Fikiet MA, Mistek E, et al. Bloodstains, paintings, and drugs: Raman spectroscopy applications in forensic science. *Forensic Chem* 2018;8:111–33.
- [63] Yan XN, Li P, Zhou B, et al. Optimal hotspots of dynamic surface-enhanced Raman spectroscopy for drugs quantitative detection. *Anal Chem* 2017;89:4875–81.
- [64] Zhao H, Hasi W, Bao L, et al. Rapid detection of sildenafil drugs in liquid nutraceuticals based on surface-enhanced Raman spectroscopy technology. *Chinese J Chem* 2017;35:1522–8.
- [65] Hong JT, Jun SW, Cha SH, et al. Enhanced sensitivity in THz plasmonic sensors with silver nanowires. *Sci Rep* 2018;8:15536.
- [66] Ding Y, Zhang X, Yin H, et al. Quantitative and sensitive detection of chloramphenicol by surface-enhanced Raman scattering. *Sensors* (Basel) 2017;17.
- [67] Saleh TA, Al-Shalalfeh MM, Al-Saadi AA. Silver loaded graphene as a substrate for sensing 2-thiouracil using surface-enhanced Raman scattering. *Sensor Actuat B-Chem* 2018;254:1110–7.
- [68] Tackman EC, Trujillo MJ, Lockwood T-LE, Merga G, Lieberman M, Camden JP. Identification of substandard and falsified antimalarial pharmaceuticals chloroquine, doxycycline, and primaquine using surface-enhanced Raman scattering. *Anal Methods* 2018;10:4718–22.
- [69] Gao J, Zhang N, Ji D, et al. Superabsorbing metasurfaces with hybrid Ag-Au nanostructures for surface-enhanced Raman spectroscopy sensing of drugs and chemicals. *Small Methods* 2018;2:1800045.
- [70] Haddad A, Comanescu MA, Green O, Kubic TA, Lombardi JR. Detection and quantitation of trace fentanyl in heroin by surface-enhanced Raman spectroscopy. *Anal Chem* 2018;90:12678–85.
- [71] Deng BE, Luo X, Zhang M, Ye LM, Chen Y. Quantitative detection of acyclovir by surface enhanced Raman spectroscopy using a portable Raman spectrometer coupled with multivariate data analysis. *Colloid Surf B-Biointerfaces* 2019;173:286–94.
- [72] Markina NE, Volkova EK, Zakharevich AM, Goryacheva IY, Markin AV. SERS detection of ceftriaxone and sulfadimethoxine using copper nanoparticles temporally protected by porous calcium carbonate. *Microchim Acta* 2018;185:8.
- [73] Meng J, Tang XH, Zhou BB, Xie QW, Yang LB. Designing of ordered two-dimensional gold nanoparticles film for cocaine detection in human urine using surface-enhanced Raman spectroscopy. *Talanta* 2017;164:693–9.
- [74] Mostowtt T, McCord B. Surface enhanced Raman spectroscopy (SERS) as a method for the toxicological analysis of synthetic cannabinoids. *Talanta* 2017;164:396–402.
- [75] Bindsri SD, Alhatab DS, Brosseau CL. Development of an electrochemical surface-enhanced Raman spectroscopy (EC-SERS) fabric-based plasmonic sensor for point-of-care diagnostics. *Analyst* 2018;143:4128–35.
- [76] Markina NE, Goryacheva IY, Markin AV. Sample pretreatment and SERS-based detection of ceftriaxone in urine. *Anal Bioanal Chem* 2018;410:2221–7.
- [77] Yu BR, Cao C, Li P, Mao M, Xie Q, Yang L. Sensitive and simple determination of zwitterionic morphine in human urine based on liquid-liquid micro-extraction coupled with surface-enhanced Raman spectroscopy. *Talanta* 2018;186:427–32.
- [78] Zhu Q, Yu X, Wu Z, Lu F, Yuan Y. Antipsychotic drug poisoning monitoring of clozapine in urine by using coffee ring effect based surface-enhanced Raman spectroscopy. *Anal Chim Acta* 2018;1014:64–70.
- [79] Berger AG, Restaino SM, White IM. Vertical-flow paper SERS system for therapeutic drug monitoring of flucytosine in serum. *Anal Chim Acta* 2017;949:59–66.

- [80] Subaihi A, Muhamadali H, Mutter ST, Blanch EW, Ellis DI, Goodacre R. Quantitative detection of codeine in human plasma using surface-enhanced Raman scattering via adaptation of the isotopic labelling principle. *Analyst* 2017;142:1099–105.
- [81] Fornasaro S, Bonifacio A, Marangon E, et al. Label-free quantification of anticancer drug imatinib in human plasma with surface enhanced Raman spectroscopy. *Anal Chem* 2018;90:12670–7.
- [82] Yue S, Sun X-T, Wang Y, Zhang W-S, Xu Z-R. Microparticles with size/charge selectivity and pH response for SERS monitoring of 6-thioguanine in blood serum. *Sens Actuators B* 2018;273:1539–47.
- [83] Litti L, Ramundo A, Biscaglia F, Toffoli G, Gobbo M, Meneghetti M. A surface enhanced Raman scattering based colloid nanosensor for developing therapeutic drug monitoring. *J Colloid Interface Sci* 2019;533:621–6.
- [84] Panikar SS, Ramírez-García G, Sidhik S, et al. Ultrasensitive SERS substrate for label-free therapeutic-drug monitoring of paclitaxel and cyclophosphamide in blood serum. *Anal Chem* 2019;91:2100–11.
- [85] Sivashanmugan K, Squire K, Ailing T, et al. Trace detection of tetrahydrocannabinol in body fluid via surface-enhanced Raman scattering and principal component analysis. *ACS Sensors* 2019;4:1109–17.
- [86] Chen Y, Li X, Yang M, et al. High sensitive detection of penicillin G residues in milk by surface-enhanced Raman scattering. *Talanta* 2017;167:236–41.
- [87] D'Elia V, Rubio-Retama J, Ortega-Ojeda FE, Garcia-Ruiz C, Montalvo G. Gold nanorods as SERS substrate for the ultratrace detection of cocaine in non-pretreated oral fluid samples. *Colloid Surf A-Physicochem Eng Asp* 2018;557:43–50.
- [88] Kodama K, Yamada K. Therapeutic drug level testing based on Raman spectroscopy of the tear fluid. 2018 11th Biomedical Engineering International Conference Biomedical Engineering International Conference, IEEE, 2018.
- [89] Souza MA, de Oliveira KV, Oliveira FCC, Silva LP, Rubim JC. The adsorption of methamphetamine on Ag nanoparticles dispersed in agarose gel – detection of methamphetamine in fingerprints by SERS. *Vib* 2018;98:152–7.
- [90] Deriu C, Conticello I, Mebel AM, McCord B. Micro solid phase extraction surface-enhanced Raman spectroscopy (mu-SPE/SERS) screening test for the detection of the synthetic cannabinoid JWH-018 in oral fluid. *Anal Chem* 2019;91:4780–9.
- [91] Hong KY, de Albuquerque CDL, Poppi RJ, Brolo AG. Determination of aqueous antibiotic solutions using SERS nanogratings. *Anal Chim Acta* 2017;982:148–55.
- [92] Khetani A, Tiwari VS, Harb A, Anis H. Monitoring of heparin concentration in serum by Raman spectroscopy within hollow core photonic crystal fiber. *Opt Express* 2011;19:15244–54.
- [93] Sieburg A, Knebl A, Jacob JM, Frosch T. Characterization of fuel gases with fiber-enhanced Raman spectroscopy. *Anal Bioanal Chem* 2019;411:7399–408.
- [94] Knebl A, Domes R, Yan D, Popp J, Trumbore S, Frosch T. Fiber-enhanced Raman gas spectroscopy for (18)O-(13)C-labeling experiments. *Anal Chem* 2019;91:7562–9.
- [95] Jochum T, Rahal L, Suckert RJ, Popp J, Frosch T. All-in-one: a versatile gas sensor based on fiber enhanced Raman spectroscopy for monitoring postharvest fruit conservation and ripening. *Analyst* 2016;141:2023–9.
- [96] Hanf S, Keiner R, Yan D, Popp J, Frosch T. Fiber-enhanced Raman multigas spectroscopy: a versatile tool for environmental gas sensing and breath analysis. *Anal Chem* 2014;86:5278–85.
- [97] Yan D, Popp J, Pletz MW, Frosch T. Fiber enhanced Raman sensing of levofloxacin by PCF bandgap-shifting into the visible range. *Anal Methods* 2018;10:586–92.
- [98] Yan D, Popp J, Pletz MW, Frosch T. Highly sensitive broadband Raman sensing of antibiotics in step-index hollow-core photonic crystal fibers. *ACS Photonics* 2017;4:138–45.
- [99] Yan D, Domes C, Domes R, et al. Fiber enhanced Raman spectroscopic analysis as a novel method for diagnosis and monitoring of diseases related to hyperbilirubinemia and hyperbiliverdinemia. *Analyst* 2016;141:6104–15.
- [100] Liu SP, Huang J, Chen Z, et al. Raman spectroscopy measurement of levofloxacin lactate in blood using an optical fiber nano-probe. *J Raman Spectrosc* 2015;46:197–201.
- [101] Yan D, Frosch T, Kobelke J, et al. Fiber-enhanced Raman sensing of cefuroxime in human urine. *Anal Chem* 2018;90:13243–8.
- [102] Azkune M, Frosch T, Arrospe E, et al. Liquid-core microstructured polymer optical fiber as fiber-enhanced Raman spectroscopy probe for glucose sensing. *J Light Technol* 2019;37:2981–8.
- [103] Frosch T, Wyrwich E, Yan D, et al. Counterfeit and standard test of the antimalarial tablet Riamet® by means of Raman hyperspectral multicomponent analysis. *Molecules* 2019;24:E3229.
- [104] Olds WJ, Sundarajoo S, Selby M, Cletus B, Fredericks PM, Izake EL. Noninvasive, quantitative analysis of drug mixtures in containers using spatially offset Raman spectroscopy (SORS) and multivariate statistical analysis. *Appl Spectrosc* 2012;66:530–7.
- [105] Moody AS, Baghernejad PC, Webb KR, Sharma B. Surface enhanced spatially offset Raman spectroscopy detection of neurochemicals through the skull. *Anal Chem* 2017;89:5688–92.
- [106] Nicolson F, Jamieson LE, Mabbott S, et al. Towards establishing a minimal nanoparticle concentration for applications involving surface enhanced spatially offset resonance Raman spectroscopy (SESORR) in vivo. *Analyst* 2018;143:5358–63.
- [107] Markin AV, Markina NE, Goryacheva IY. Raman spectroscopy based analysis inside photonic-crystal fibers. *TrAC Trends Anal Chem* 2017;88:185–97.
- [108] Brückner M, Becker K, Popp J, Frosch T. Fiber array based hyperspectral Raman imaging for chemical selective analysis of malaria-infected red blood cells. *Anal Chim Acta* 2015;894:76–84.
- [109] Yan D, Popp J, Frosch T. Analysis of fiber-enhanced Raman gas sensing based on Raman chemical imaging. *Anal Chem* 2017;89:12269–75.
- [110] Tran V, Walkenfort B, König M, Salehi M, Schlucker S. Rapid, quantitative, and ultrasensitive point-of-care testing: a portable SERS reader for lateral flow assays in clinical chemistry. *Angew Chem -Int Edit* 2019;58:442–6.
- [111] Olds WJ, Jaatinen E, Fredericks P, Cletus B, Panayiotou H, Izake EL. Spatially offset Raman spectroscopy (SORS) for the analysis and detection of packaged pharmaceuticals and concealed drugs. *Forensic Sci Int* 2011;212:69–77.
- [112] Matousek P, Clark IP, Draper ER, et al. Subsurface probing in diffusely scattering media using spatially offset Raman spectroscopy. *Appl Spectrosc* 2005;59:393–400.

- [113] Zhang X, Wang S, Li J, et al. Study on a non-destructive drug testing method based on spatially offset Raman spectroscopy. *Spectrosc Spectr Anal* 2019;39:1472–6.
- [114] Stokes RJ, Bailey M, Bonthorn S, et al. In: Optics and photonics for counterterrorism, crime fighting, and defence XII. 999506 (International Society for Optics and Photonics).
- [115] Matousek P, Stone N. Development of deep subsurface Raman spectroscopy for medical diagnosis and disease monitoring. *Chem Soc Rev* 2016;45:1794–802.
- [116] Stone N, Faulds K, Graham D, Matousek P. Prospects of deep Raman spectroscopy for noninvasive detection of conjugated surface enhanced resonance Raman scattering nanoparticles buried within 25 mm of mammalian tissue. *Anal Chem* 2010;82:3969–73.
- [117] Zachhuber B, Östmark H, Carlsson T. Spatially offset hyperspectral stand-off Raman imaging for explosive detection inside containers. Vol. 9073 SID (SPIE, 2014).
- [118] Kiefer J, Noack K. Universal enantioselective discrimination by Raman spectroscopy. *Analyst* 2015;140:1787–90.
- [119] Rullich CC, Kiefer J. Chemometric analysis of enantioselective Raman spectroscopy data enables enantiomeric ratio determination. *Analyst* 2019;144:5368–72.
- [120] Rullich CC, Kiefer J. Enantioselective Raman spectroscopy (esR) for distinguishing between the enantiomers of 2-butanol. *Analyst* 2018;143:3040–8.
- [121] Rullich CC, Kiefer J. Principal component analysis to enhance enantioselective Raman spectroscopy. *Analyst* 2019;144:2080–6.
- [122] Sun M, Zhang Z, Wang P, Li Q, Ma F, Xu H. Remotely excited Raman optical activity using chiral plasmon propagation in Ag nanowires. *Light Sci Appl* 2013;2:e112–e112.
- [123] Gasiór-Głogowska M, Malek K, Zajac G, Baranska M. A new insight into the interaction of cisplatin with DNA: ROA spectroscopic studies on the therapeutic effect of the drug. *Analyst* 2016;141:291–6.
- [124] Barron LD. The development of biomolecular Raman optical activity spectroscopy. *Biomed Spectrosc Imaging* 2015;4:223–53.
- [125] Thiagarajan G, Widjaja E, Heo JH, et al. Use of Raman and Raman optical activity for the structural characterization of a therapeutic monoclonal antibody formulation subjected to heat stress. *J Raman Spectrosc* 2015;46:531–6.
- [126] Abdali S, Blanch EW. Surface enhanced Raman optical activity (SEROA). *Chem Soc Rev* 2008;37:980–92.
- [127] Ostovar Pour S, Rocks L, Faulds K, et al. Through-space transfer of chiral information mediated by a plasmonic nanomaterial. *Nat Chem* 2015;7:591–6.
- [128] Wu T, Zhang X, Wang R, Zhang X. Strongly enhanced Raman optical activity in molecules by magnetic response of nanoparticles. *J Phys Chem C* 2016;120:14795–804.
- [129] Aaltonen J, Gordon KC, Strachan CJ, Rades T. Perspectives in the use of spectroscopy to characterise pharmaceutical solids. *Int J Pharm* 2008;364:159–69.
- [130] Fornasaro S, Dalla Marta S, Rabusin M, Bonifacio A, Sergio V. Toward SERS-based point-of-care approaches for therapeutic drug monitoring: the case of methotrexate. *Faraday Discuss* 2016;187:485–99.
- [131] Zhu Q, Cao Y, Cao Y, Chai Y, Lu F. Rapid on-site TLC–SERS detection of four antidiabetes drugs used as adulterants in botanical dietary supplements. *Anal Bioanal Chem* 2014;406:1877–84.
- [132] Yang T, Guo X, Wang H, Fu S, Wen Y, Yang H. Magnetically optimized SERS assay for rapid detection of trace drug-related biomarkers in saliva and fingerprints. *Biosens Bioelectron* 2015;68:350–7.
- [133] Wang B, Xu X. Based on Raman spectroscopy for trace drug illegal additives for detection method [Machine Translation]. CN107907525A (2018).
- [134] Dana K, Shende C, Huang H, Farquharson S. Rapid analysis of cocaine in saliva by surface-enhanced Raman spectroscopy. *J Anal Bioanal Tech* 2015;6:1–5.
- [135] Inc, T. F. S. Using handheld Raman spectroscopy: synthetic marijuana: field identification of bulk and sprayed cannabinoids. *TECHNICAL NOTE No. 202a* (2018).
- [136] Sivashanmugan K, Squire K, Tan A, et al. Trace detection of tetrahydrocannabinol in body fluid via surface-enhanced Raman scattering and principal component analysis. *ACS Sensors* 2019;4:1109–17, doi:10.1021/acssensors.9b00476.